Journal of Environmental Science International
22(4); 407~413; April 2013

pISSN: 1225-4517 eISSN: 2287-3503
http://dx.doi.org/10.5322/JESI.2013.22.4.407

ORIGINAL ARTICLE

A Study of a Hydrophobic Surface: Comparing Pure Water and Contaminated Water

Matthew Stanley Ambrosia*, Chang-Han Lee

College of Applied Sciences, Catholic University Pusan, Busan 609-757, Korea

Abstract

The flow of sewage has been studied for hundreds of years. Reducing drag in pipes can allow sewer to be removed easily and quickly. Drag reduction is not only a macroscale issue. Physical and chemical properties of the nano-scale can affect flow at the macroscopic scale. In this paper the predictability of hydrophobicity at the nano-scale is studied. Molecular dynamics simulations were used to calculate the range of contact angles of water droplets in equilibrium on a pillared graphite surface. It was found that at a pillar height of two graphite layers there was the largest range of contact angles. It is observed that at this height the droplet begins to transition from the Wenzel state to the Cassie-Baxter state. Surfaces with larger pillar heights have much larger contact angles corresponding to a more hydrophobic surface. Silicon dioxide was also simulated in the water droplet. The contaminant slight decreased the contact angle of the water droplet.

Key words : Molecular dynamics, Hydrophobic, Contact angle, Water droplet, Silicon dioxide

1. Introduction

The sewage flow is increasingly becoming a more important issue with the population of the earth growing exponentially. Population densities are growing in urban areas which means the sewage flow per square kilometer is increasing so there needs to be a more efficient use of space. Increasing the flow of sewage by reducing drag in pipes has been studied recently. Ptasinski et al.(2001). conducted a study on the reduction of drag in turbulent pipe flow using polymer additives. Depending on the concentration of these polymer additives experiments show drag reduction can be reduce up to 60 - 70%. More recently focus has turned to nano-scale pipe coating. Liu et al.(2011). recorded a 10% pressure drop reduction and a temperature reduction of 2.5 - 5°C in an oil pipeline. They coated the inner wall of the pipeline with a nanometer coating with effectively decreased the surface energy of the inner wall of the pipeline making it more oleophobic.

Reducing the effective surface energy of a surface is a good way to increase hydrophobicity. Surfaces with contact angles smaller than 90° are considered hydrophilic while surfaces with contact angles of more than 90° is considered hydrophobic. It has been known that surface texture at multiple scales increases hydrophobicity. Gao and McCarty(2006) explained the reason why even nano-scale texture increases hydrophobicity. On staggered rhombus pillars they applied a polymernanoscale coating which had no apparent hysteresis, difference between

Received 29 March, 2013; **Revised** 8 April, 2013;
Accepted 18 April, 2013
***Corresponding author** : Matthew Stanley Ambrosia, College of Applied Sciences, Catholic University Pusan, Busan 609-757, Korea
Phone: +82-10-7740-0076
E-mail: ambrosia@cup.ac.kr

the advancing and receding contact angle, which is an indicator of a highly hydrophobic surface.

There are two major types of wetting phenomenon observed on textured surfaces. Water droplets that completely wet the textured surface are in the Wenzel(1936) state. In other cases water droplets sit on top of the textured surface only touching a fraction of the surface below it. This case was identified by Cassie and Baxter(1944). The Cassie and Wenzel states can be seen in Fig. 1.

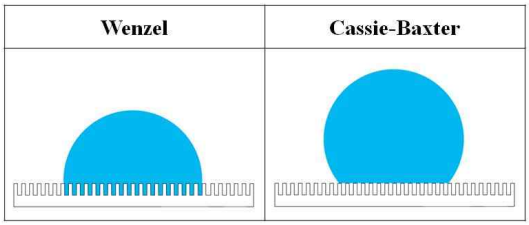

Fig. 1. Droplet in the Wenzel state and the Cassie-Baxter state.

At the nano-scale molecules are continuously moving and any surface may have a range of contact angles. In this paper molecular dynamics simulations were used to find the range of contact angles of a nano-sized water droplet on a pillared graphite surface. Jeong et al.(2012) presented contact angles for a water droplet on pillared graphite surfaces like the surface used in this study without uncertainties. This study will evaluate a possible range of uncertainty for these values. Silicon dioxide was also inserted into the water droplet and its effect on the water droplet's contact angle was recorded.

2. Materials and Methods

The parallel molecular dynamics simulation program called NAMD(Philips et al., 2005) was used to trace the movement of a water droplet on a pillared graphite surface. Molecular dynamics simulations model the actual movement of atoms by calculating the sum of the different forces on those atoms and solving the Newton's equations of motion using the velocity Verlet algorithm with a time step of 2.0 fs. To calculate those forces, the position of each atom is needed along with the interacting bonded and non-bonded forces. The bonded forces include atomic bonds and angles between atoms. Non-bonded potentials include the Lennard-Jones and electrostatic potentials. The Lennard Jones potential, V_{LJ} accounts for the van der Waals forces attracting and repelling atoms depending on the distance r_{ij} between the two atoms and can be calculated using Equation 1.

$$V_{LJ} = \varepsilon_{ij}\left[\left(\frac{R_{\min}}{r_{ij}}\right)^{12} - \left(\frac{R_{\min}}{r_{ij}}\right)^{6}\right] \quad (1)$$

whereε_{ij} and $R_{min}$are the characteristic surface energy and van der Waals radius, respectively.

The long-range electrostatic interactions were calculated using the Ewald(1921) method. As the distance between atoms increase the Lennard-Jones potential quickly approaches 0 and is truncated at a cutoff radius of 12 Å with a smoothing function turned on at a switching distance of 10 Å.

A NVT ensemble was used, which holds the number of atoms, volume and temperature constant as the simulations were run. The temperature was set to 298.15K and controlled using the velocity scaling method as calculations were being made on 5124 TIP3P water molecules. In the TIP3 water model the O-H bonds are 0.9572 Å in length and has three charges, -0.834 e for the O atom and +0.417 e for the H atoms with an angle of 104.52 degrees between the atoms.

The (0001) graphite surface was chosen for its hexagonal tabular structure and it was fixed spatially to reduce computational time. Its dimensions were $L_x \times L_z$ = 145 Å × 145 Å or larger with periodic boundaries in each direction. The pillar's lateral

dimensions were $P_x \times P_z$= 8.51 Å × 7.37 Å and the gaps between the pillars were $G_x \times G_z$= 8.51 Å × 7.37 Å with a pillar height of *H*. These pillar-gap dimensions can be seen in Fig. 2. Using graphite as the surface restricts the pillar height to be multiples of 3.35 Å because this is the distance by which adjacent graphite layers are spaced. In this study five different pillar heights ranging from 1 graphite layer to 5 graphite layers were considered to evaluate the contact angles. A pillar height of 1 will refer to a pillar with only one graphite layer (3.35 Å). A pillar height of 2 will refer to a pillar with two graphite layers (6.70 Å) and so on. The y-direction of the domain was at least 145 Å to ensure that it was large enough so that there were no significant interactions in the y-direction beyond the boundary.

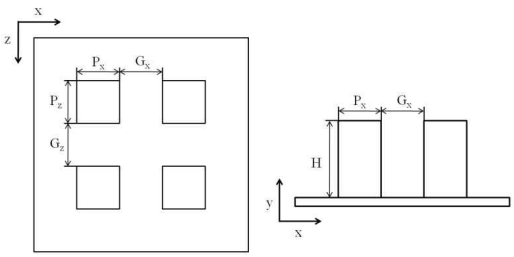

Fig. 2. Profile and top schematic of the pillar and gap dimensions.

To calculate the time averaged contact angles for the water droplet, the water molecule simulations ran for 10 ns. Even after equilibrium is reached movement of the molecules cause slight variations in the droplet's contact angles. Therefore, during the last 2 ns of the simulation, contact angles were calculated on four sides of the droplet every 5 ps and then all the contact angles extracted were averaged. The contact angle is defined as the angle between two lines. Line-1 is from the edge of the droplet on the top surface of the pillar to the center of mass projected on the pillar surface top. Line-2 is from the edge of the droplet at the top of the pillar surface along the line measuring a normalized 50 % density of water molecules at the edge of the water droplet. Fig. 3 shows the density profile of a droplet and its contact angle. The contact angle was measured using the least-squares fitting of circles method suggested by Gander et al.(1994).

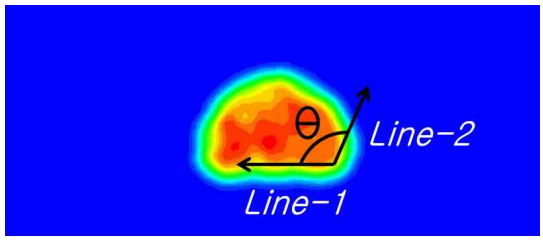

Fig. 3. Snapshot of water droplet density profile and contact angle between Line-1 and Line-2.

To validate the graphite surface for the molecular dynamics simulations the characteristic surface energy was chosen so that the contact angles of the simulations and experimental results matched. Fowkes and Harkins(1940) conducted experiments and found that on flat graphite surfaces contact angles ranged from 85.3° to 85.9°. The characteristic surface energy of -0.0385 kcal/mol and a van der Waals radius of 1.9924 Å for the flat graphite surface gave a time averaged contact angle of 85.9° agreeing well with the experimental results.

Molecular dynamics simulations using parallel processors are not perfectly repeatable. At the start of the simulation atomic velocities are randomized following the Gaussian distribution corresponding to the specific temperature. Each particle will be given a different velocity according to a random number generator. In addition to this, as simulations are run using parallel computing different tasks are assigned to different processors and then combined. This may also cause slight variations in the results like the "butterfly effect" especially for cases with a large number of atoms and/or when simulations are carried out over thousands even millions of time steps.

However regardless of the variations of the results, they all are in the range of physical possibility.

A contaminate was introduced to a pure water droplet composed of 5,124 molecules of H_2O in the defined dimension of $L_x \times L_y \times L_z$ = 145 Å × 145 Å × 145 Å. Contaminated water is considered to have 0.5 g/L. In our calculations we used a droplet made up of 10 times the sewage concentration on the assumption that it has a lot of suspended solid as its contaminant which is 5.0 g/L of only a constituent of SiO_2.

1L of water solution has a density of 0.997 kg/Lat 25° C and a molecular weight of 55.08 mol/g. 5.0 g of SiO_2 with a molecular weight of 60.07 mol/gis calculated to be 0.0823 mol of SiO_2. The SiO_2/H_2O molar ratio is 1.5111×10^{-3} mol. Therefore the calculated number of SiO_2 molecules is 7.7427 per 5,124 water molecules. To simulate these conditions we inserted8 molecules of SiO_2 into the water droplet and simulations were run for 10 ns.

In this study molecular dynamics simulations under identical conditions were repeated to find a range of possible contact angles for a nano-sized pure water droplet on a pillared graphite surface. Also simulations were run on a contaminated water droplet to compare its contact angle to the range of contact angles of the pure water.

3. Results

Molecular dynamics simulations were run ten times for each pillar height and the contact angles were calculated and recorded. The initial positions of the 5124 water molecules were in the form of a cube with dimensions of approximately 50 Å on each side. An example of the starting position is found in Fig. 4.

In Fig. 5 snapshots of droplets in equilibrium for each pillar height can be seen. Droplets on the surface with a pillar height of 1 and 2 (Fig. 5(a) and 5(b), respectively) are in the Wenzel state wetting the entire surface and the other droplets are in the more hydrophobic Cassie-Baxter state sitting on top of the textured surface.

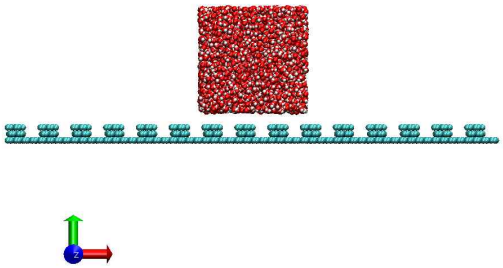

Fig. 4. An Example of the initial position of the water molecules above the pillared surface before simulations begin.

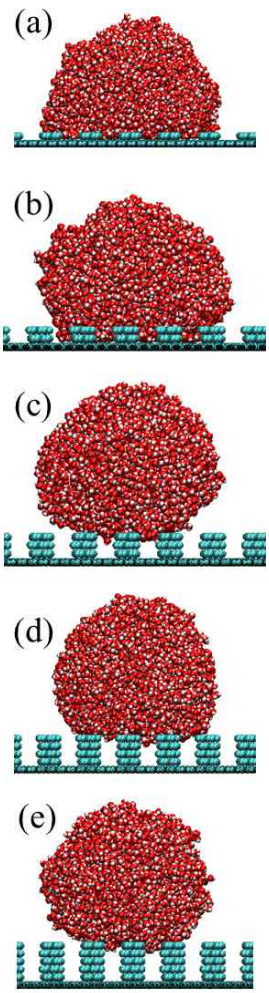

Fig. 5. Snapshots of droplets at equilibrium at a pillar height of (a) 1, (b) 2, (c) 3, (d) 4, and (e) 5.

In this study simulations were carried out for 10 ns and the contact angles around the droplet were averaged over the last 2 ns to get an accurate measurement of the contact angle for each case. The average of the contact angles of all the trials simulated along with the minimum, maximum and range of contact angles can be found in Table 1. As seen in previous studies as the pillar height increases contact angles get larger and the surface becomes more hydrophobic until the Cassie-Baxter state is reached. When the droplet is in the Cassie-Baxter state the pillar height has little effect on the contact angle on the droplet. For all the pillar heights we see a range of contact angles from 3.4° to 11.2°. The largest range is at the pillar height of 2 which is the tallest pillar height the droplet is in the Wenzel state. The large range of contact angles at this pillar height is due to the transition between the Wenzel state to the Cassie-Baxter state. The droplet is in a less stable state and fluctuates in shape and may have several semi-equilibrium states as the droplet tries to pull the water out from between the pillar due to its surface tension. The droplets in the Cassie-Baxter state (pillar heights 3, 4, 5) have the smallest range of contact angles of the pillar heights.

Table 1. Average, minimum, maximum, and range of contact angles for the ten trials

Pillar Height	Average	Min	Max	Range
1	108.6°	106.7°	113.6°	6.9°
2	122.2°	115.4°	126.6°	11.2°
3	132.6°	129.6°	135.2°	5.6°
4	134.6°	132.8°	136.2°	3.4°
5	132.6°	129.5°	134.3°	4.9°

In Fig. 6 contact angles for the trials of this present study as well as the contact angles published by Jeong et al.(2012). They ran simulations for 5 ns and conducted time averaging over the last 2 ns. In the present study simulations ran for 10 ns and the contact angles were calculated and averaged over the last 2 ns. Most of the contact angles in the previous study are within the range of the present study. However at a pillar height of 2 the contact angle of Jeong et al.(2012) were higher. At the pillar height of 2 the droplet appears to take longer to reach equilibrium than at other pillar heights. This is due to the unstable nature of the droplet on this surface since it is just one layer away from transition to the Cassie-Baxter state.

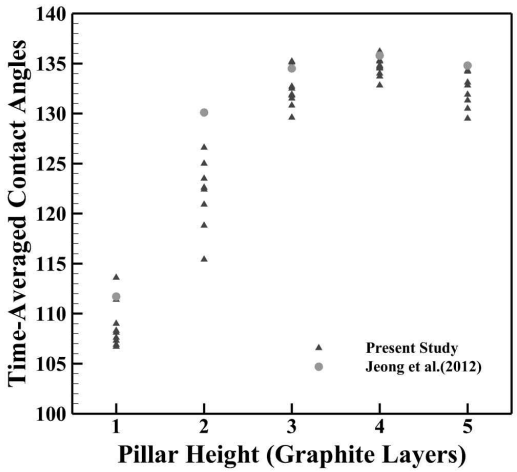

Fig. 6. Contact angles of the trails of this present study compared to the contact angles found in the study of Jeong et al.(2012).

Eight SiO_2 molecules were inserted into the initial water droplet for the pillar height of four to evaluate the effect of contaminants in the water droplet on the contact angle. Fig. 7 shows the contaminated water droplet in equilibrium with the pillared surface. As time advanced eventually all of the SiO_2 molecules left the water droplet and most of them moved to the graphite surface. This occurred because the surface energy of SiO_2 is stronger than the water molecule and therefore is more attracted to the surface. The time-averaged contact angle for the contaminated water droplet was 132.2°. These results are 2.4° lower than the average contact angle for pure water

and 0.6° below the minimum contact angle for the same surface with pure water. Therefore the contaminants, even though they left the water droplet, made the water droplet more hydrophilic. It seems that the SiO_2 molecules will affect the flow of the contaminated water also making it more difficult to flow compared to pure water.

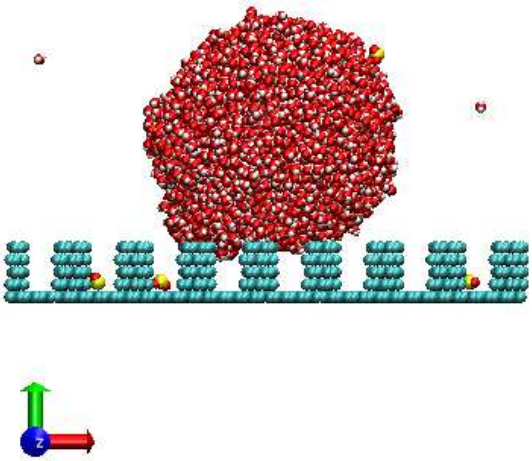

Fig. 7. Water droplet with SiO_2 molecules.

4. Conclusions

In this paper molecular dynamics simulations were run for water droplets on graphite surfaces with different pillar heights. Ten trails were run for each pillar height and contact angles were calculated around the droplet and averaged for each trial. Each droplet in equilibrium were classified into either the Wenzel state or the Cassie-Baxter state. The range of contact angles were from 3.4° to 11.2°. At a pillar height of 2 the largest range was found. It was observed that the pillar height of 2 is the largest pillar height at which the droplet is in the Wenzel state. The large range of contact angles is attributed to the droplet in an unstable state where it will transition to the Cassie-Baxter state if the pillar height is raised one more level. Droplets in the Cassie-Baxter state were found to have a smaller range of contact angles meaning it is easier to predict the hydrophobicity of these surfaces. Contaminants (SiO_2) were introduced to the water droplet and caused the water droplets contact angle to decrease slightly for the conditions simulated. Therefore the flow of sewage on surfaces and in pipes is also expected to flow slower compared to pure water under the same conditions.

It is also suggested not any nano-texture on the inner surface of pipes will optimize flow and reduce drag. When considering nano-textures for the inner surface of pipes the surface should be rough enough to ensure the fluid does not completely wet the surface as in the Wenzel cases. Surfaces with taller pillar-like nano-textures as in the Cassie Baxter state tend to be hydrophobic and more predictable in the area of hydrophobicity.

Acknowledgements

This study was made possible thanks to the 2011 research funding from the Catholic University of Pusan.

References

Cassie, A. B. D., Baxter, S.,1944, Wettability of porous surfaces, Trans. Faraday Soc., 40, 546-551.

Ewald, P. P., 1921, Die Berchnungoptischer und elektrostatischer Gitterpotentiale, Annalen der Physik, 64, 253-287.

Fowkes, F. M., Harkins, W. D., 1940, The State of Monolayers Adsorbed at the Interface Solid-Aqueous Solution, J. Am. Chem. Soc., 62, 3377-3386.

Gander, W., Golub, J. H., Strebel, R., 1994, Least-squares fitting of circles and ellipses, BIT, 34, 558-578.

Gao, L., McCarthy, T. J., 2006, The “Lotus Effect” Explained: Two Reasons Why Two Length Scales of Topography Are Important, Langmuir, 22, 2966-2967.

Jeong, W. J., Ha, M. Y., Yoon, H. S., Ambrosia, M., 2012, Dynamic Behavior of Water Droplets on

Solid Surfaces with Pillar-Type Nanostructures, Langmuir, 28, 5360-5371.

Liu, B., Zong, Z., Wang, P., Du, H., 2011, Experimental Study on Water Cut Oil Flowing in Nanometer Coated Pipeline, Proceedings of ICPTT, ASCE, Beijing, 523-531.

Ptasinski, P. K., Nieuwstadt, F. T. M., Van Den Brule, B. H. A. A., Hulsen M. A., 2001, Experiments in Turbulent Pipe Flow with Polymer Additives at Maximum Drag Reduction, Flow, Turbulence and Combustion, 66, 159-182.

Phillips, J. C., Braun, R., Wang, W., Gumbart, J., Tajkhorshid, E., Villa, E., Chipot, C., Skeel, R. D., Kale, L., Schulten. K., 2005, Scalable molecular dynamics with NAMD,J. Comput. Chem., 26, 1781-1802.

Wenzel, R. N., 1936, Resistance of solid surfaces to wetting by water, Ind. Eng. Chem., 28, 988-994.